Author(s): Putkonen, Matti; Heikkilä, Pirjo; Pasanen, Antti T.; Rautkoski, Hille; Svärd, Laura; Simell, Pekka; Vähä-Nissi, Mika; Sajavaara, Timo

Title: Atomic layer deposition of Ti-Nb-O thin films onto electrospun fibers for fibrous and tubular catalyst support structures

Year: 2018

Version:

Please cite the original version:

Putkonen, M., Heikkilä, P., Pasanen, A. T., Rautkoski, H., Svärd, L., Simell, P., Vähä-Nissi, M., & Sajavaara, T. (2018). Atomic layer deposition of Ti-Nb-O thin films onto electrospun fibers for fibrous and tubular catalyst support structures. Journal of Vacuum Science and Technology A, 36(1), Article 01A102. https://doi.org/10.1116/1.4999826

Atomic layer deposition of Ti-Nb-O thin films onto electrospun fibers for fibrous and tubular catalyst support structures

Matti Putkonen, Pirjo Heikkilä, Antti T. Pasanen, Hille Rautkoski, Laura Svärd, Pekka Simell, Mika Vähä-Nissi, and Timo Sajavaara

Citation: Journal of Vacuum Science & Technology A: Vacuum, Surfaces, and Films **36**, 01A102 (2018);

View online: https://doi.org/10.1116/1.4999826

View Table of Contents: http://avs.scitation.org/toc/jva/36/1

Published by the American Vacuum Society

Atomic layer deposition of Ti-Nb-O thin films onto electrospun fibers for fibrous and tubular catalyst support structures

Matti Putkonen,[a] Pirjo Heikkilä, Antti T. Pasanen, Hille Rautkoski, Laura Svärd, Pekka Simell, and Mika Vähä-Nissi
VTT Technical Research Centre of Finland, P.O. Box 1000, 02044 VTT Espoo, Finland

Timo Sajavaara
Department of Physics, University of Jyväskylä, P.O. Box 35, FI-40014 Jyväskylä, Finland

(Received 11 August 2017; accepted 2 October 2017; published 30 October 2017)

Here, the authors report on the preparation of core–shell carbon-ceramic fibrous as well as ceramic tubular catalyst supports utilizing electrospinning and atomic layer deposition (ALD). In this paper, ALD of Ti-Nb-O thin films using $TiCl_4$, $Nb(OEt)_5$, and H_2O as precursors is demonstrated. According to the time-of-flight-elastic recoil detection analysis and Rutherford backscattering spectrometry, carbon and hydrogen impurities were relatively low, but depend on the pulsing ratio of the precursors. Optimized ALD process was used for coating of sacrificial electrospun polyvinyl alcohol (PVA) template fibers to yield tubular Ti-Nb-O structures after thermal or solution based PVA removal. Another approach utilized 200–400 nm thick carbon fibers prepared by electrospinning from polyacrylonitrile and subsequent thermal treatment. *Published by the AVS.*
https://doi.org/10.1116/1.4999826

I. INTRODUCTION

Electrocatalyst support materials for proton-exchange membrane (PEM) fuel cells require high electronic conductivity, high specific surface area, and high stability. Conventional support structures typically consist of Pt particles on carbon black. However, the use of carbon without a protective layer is limited at high cell potentials due to oxidative corrosion. Several studies on PEM fuel cell research have been carried out to tackle the corrosion issues based on either developing new noncarbon catalyst support materials or modifying the existing carbon supports.[1] Alternative materials such as carbon nanotubes,[2] ITO,[3] metal carbides,[4] SnO_2,[5,6] ZrO_2,[7] Nb_2O_5,[8,9] TiO_2,[10,11] and Nb-TiO_2 (Ref. 12) have been studied as support materials. The second approach is to improve the existing carbon support materials against corrosion by using dopants such as nitrogen,[13] WC,[14] and MnO_2 (Ref. 15) on carbon matrix. Only recently, carbon supports are being modified by the preparation of core–shell structures of Pt/NbO_2/CNT by sputtering.[16] Also, liquid phase methods are applied to coat CNT bundles by SnO_2.[17]

Atomic layer deposition (ALD) is a variant of conventional chemical vapor deposition method in which the reactive precursors are supplied sequentially. ALD is especially suitable for the preparation of nanoscale materials on the three-dimensional structures where exact film conformality is needed. A variety of ALD materials have also been previously deposited onto the carbon substrates and carbon nanotubes.[18] Since sp^2-hybridized carbon materials such as CNTs, graphene, and HOPG are relatively inert compared to the conventional hydroxide terminated substrates, functionalization prior deposition is often needed to obtain smooth films. Different noncovalent and covalent approaches have been developed in order to obtain smooth films. However, defects and surface sites on carbon fibers and carbon nanotube surfaces enable direct deposition without any pretreatment.

Here, we have been using ALD for conformal protective layers on electrospun high surface area carbon fiber webs. The selection of coating was determined by the fact that the protective layer should not increase the resistivity higher than commercial Vulcan carbon, which has conductivity around 4 S cm^{-1}. In general, many oxide membrane electrode assemblies (MEAs) offer improved electrochemical and thermal stabilities but have insufficient electrical conductivity. For example, TiO_2 fibers have been tested for MEA structures, but the resistivity is too high for PEM MEAs, being 0.132 and 0.124 S cm^{-1} for anatase and rutile, respectively. A significant increase in film conductivity has also been observed with ALD deposited Ti-Nb-O compared to the TiO_2 alone. Planar ALD films deposited from $Ti(OMe)_4$, $Nb(OEt)_5$, and H_2O can be crystallized by forming gas annealing and converting them from nearly insulating films to relatively well conducting with resistivities around 2–10 mΩ cm.[19] Oxide layer providing protection for carbon fibers is also beneficial acting as tie-layer for subsequent platinum deposition using ALD methods.[20]

In this paper, we report on the ALD of Ti-Nb-O thin films to be used as a tie-layer in the PEM fuel cell catalyst carrier. This is done by using a slightly different precursor combination that was reported earlier by using $TiCl_4$, $Nb(OEt)_5$, and H_2O as precursors. We made initial depositions onto silicon and borosilicate glass reference surfaces and then transferred the ALD process on two types of electrospun fibers: carbonized fibers for the production of core–shell structures and sacrificial template fiber for the production of tubular structures.

II. EXPERIMENT

In our study, Ti-Nb-O films were deposited by ALD technique by using $Nb(OEt)_5$ and $TiCl_4$ and H_2O as precursors.

[a]Electronic mail: matti.putkonen@vtt.fi

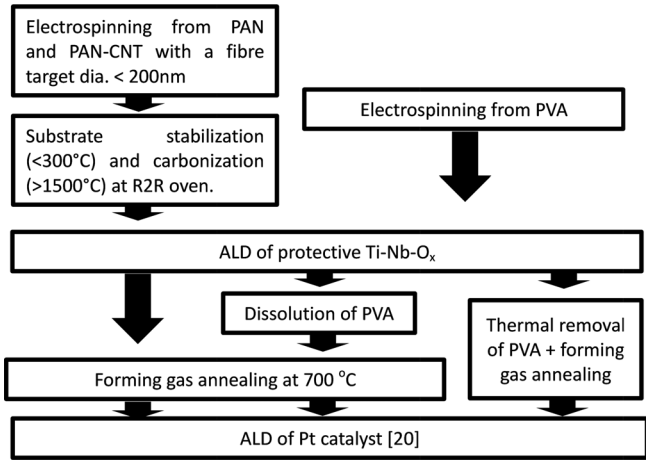

FIG. 1. Schematic overview of the catalyst support preparation by using electrospinning and ALD.

In the first stage, the films were deposited onto reference (100) silicon and borosilicate glass (Duran) in order to study the growth process and film properties and later on to high surface area electrospun webs. ALDs were carried out by using Picosun R-200 ALD tool set up for the single wafer depositions. The deposition temperature was kept constant at 175 °C. $Nb(OEt)_5$ was evaporated from Picohot 300 hot source at 130–140 °C. $TiCl_4$ was kept at 18 °C for sufficient vapor pressure to obtain surface saturation during precursor pulsing. In order to study the effect of Nb:Ti precursor ratio on the film composition and conductivity, sample series with a varied precursor pulsing ratio were deposited.

The deposited films were analyzed first by using a ellipsometer in order to determine the film's growth rate, uniformity, and refractive index (Sentech 400 ADV @ 587 nm). The composition of the selected thin film samples on silicon substrates was determined using time-of-flight-elastic recoil detection analysis (TOF-ERDA).[21,22] In this method, a heavy 11.9 MeV $^{63}Cu^{6+}$ ion beam is directed to the sample and the time of flight (velocity) and energy of recoiled sample atoms are measured with a detector telescope at 41° to the beam direction. Independent measurement of the velocity and energy of recoil atoms allows them to be differentiated according to their mass. The elemental depth profiles were determined by means of known geometry, elastic scattering cross-sections, and stopping forces.[23] The chlorine content of the selected thin film samples was determined using Rutherford backscattering spectrometry (RBS) with a 2 MeV $^4He^+$ ion beam backscattered at 165°. The 2 mm diameter beam was incident at 7° to the sample surface normal. The SIMNRA simulation program[24] was used to obtain the elemental ratios by comparison of simulated and experimental RBS spectra.

Two different approaches were tested in order to make high surface area support structures. Schematics of the process flow are presented in Fig. 1. First, the tubular structures are produced via the "tubes-using-fiber-templates" (TUFT) method[25] consisting of three stages. For the production of sacrificial template fibers, two polyvinyl alcohol (PVA) grades, PVA_{High} from Merck (Mw 200 000, partly hydrolyzed >85%) and PVA_{Low} from Aldrich (Mw 10 000, partly hydrolyzed 80%), were first mixed and then used for electrospinning. Typical electrospinning parameters and obtained fiber diameters are listed in Table I. These fibers were collected as sheets, which were then ALD coated with Ti-Nb-Ox. Tubular structures were obtained either by the removal of polymer by thermal treatment or by dissolution to obtain nanostructural tubes. The coated fibers were immersed into 100 °C water for 0.5–3 h in order to dissolve PVA. The tubes were then heat-treated in order to obtain a conductive support material.

The second approach is based on the electrospinning of polyacrylonitrile (PAN) (Mw ~ 200 000, from Good Fellow). Self-sustaining sheets were collected, and PAN sheets were stabilized at 260–270 °C and carbonized at 1500 °C; for more details, see Ref. 20. After carbonization, optimized ALD process was used to coat carbon webs with dimensions ~200 × 100 mm^2 in a stop-flow mode. After Ti-Nb-O film deposition, coated webs were annealed at 700 °C in forming gas (4% H_2 in Ar) for 30 min in order to crystallize films and obtain conductive phase. Conductivity was measured by using four-point resistance measurements by an in-house developed probe. X-ray diffraction (XRD) device PANalytical X'Pert Powder PIXcel1D was used to examine the crystal structure of the support material both before and after annealing. SEM imaging of sheets with JEOL JSM 6360LV and Zeiss Merlin FEG-SEM was done for determining the fiber structure and fiber diameters. The fiber diameters were determined from the SEM images by calculating an average of at least 50 single fiber diameters measured using ISOLUTION LITE or IMAGE J (Ref. 26) programs.

III. RESULTS AND DISCUSSION

Previously, Nb_2O_5 has been deposited by ALD using mainly either $NbCl_5$ (Refs. 27 and 28) or $Nb(OEt)_5$ (Ref. 29)

TABLE I. Experimental details of fiber preparation.

Process	Electrospinning solution	Electrospinning setup	Electrospinning parameters (voltage, distance, nozzle size, and feed flow)	Typical fiber (diameters/nm)
PAN for carbon fibers	6.6–7 wt. % in *N*,*N*-dimethylformamide	Eltex KNH64; rotating collector with moving nozzle	12–15 kV; 10–15 cm; 17 G; 0.7 ml/h	PAN 160–440 nm, stab. 200–270 nm, carbon 160–200 nm
Sacrificial PVA for tubular structure	7 wt. % in H_2O	Simco CM5-30P	23 kV; 13 cm; 19 G	PVA ∅ = 360 ± 70 nm

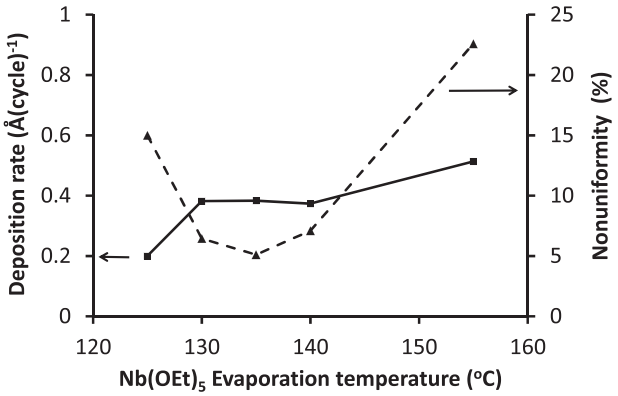

FIG. 2. Nb_2O_5 film deposition rate and film uniformity as a function of $Nb(OEt)_5$ evaporation temperature.

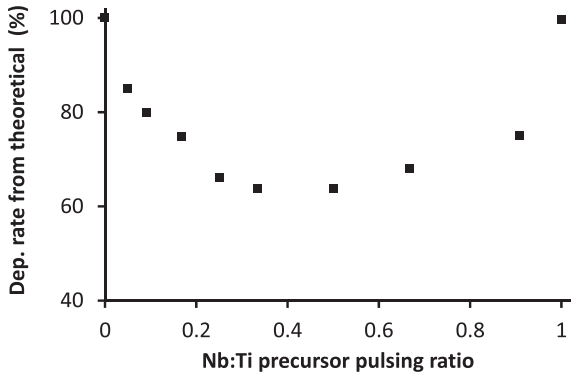

FIG. 4. Ti-Nb-O deposition rate as a function precursor pulsing ratio. Pulsing ratios of 0% and 100% represent deposition rates of 0.5 and 0.38 Å/cycle for binary TiO_2 and Nb_2O_5 at 175 °C, respectively.

as a metal precursor. $NbCl_5$ is having a tendency to etch Nb_2O_5 (Ref. 28) leading to nonuniform films so most of the reported processes are relying on $Nb(OEt)_5$ as like previously published process for Ti-Nb-O.[19] In that report, $Ti(OMe)_4$ was used as titanium precursor instead of common $TiCl_4$ in order to avoid HCl formation and possible film contamination. Our target was to be prepared for scaling of the Ti-Nb-O processes for industrial size high surface area substrates, so the use of $TiCl_4$ as a precursor was evaluated since it has been also previously used successfully for industrial-scale ALD processes.[30]

It is known that evaporation temperatures of 130–140 °C are sufficient to provide surface saturation during film growth with binary Nb_2O_5 deposition rate of 0.38 Å/cycle. Since purging times were kept constant at 5 s, CVD type growth was observed when evaporation temperature was over 155 °C indicating excess precursor dose (Fig. 2). For the following depositions, $Nb(OEt)_5$ temperature was kept at 135 °C. In the next set of experiments, $TiCl_4 + H_2O$ cycle was combined with $Nb(OEt)_5 + H_2O$ process. ALD type growth was verified by using $TiCl_4$+H_2O: $Nb(OEt)_5$+H_2O ratio of 2:1 and increasing the $TiCl_4$ pulse length (Fig. 3).

The deposition rate was dependent on the metal precursor pulsing ratio. Deposition rates for binary TiO_2 and Nb_2O_5 were 0.5 and 0.38 Å/cycle, respectively. When mixed oxides were deposited, a decrease in the overall growth rate was observed (Fig. 4), the deposition rate being lowest of around 65% when calculated from binary oxide deposition rates. The change in the growth rate is a typical phenomenon for ternary oxide materials deposited by ALD often explained by etching[31] or different amount of reactive sites compared to the binary films.[32] Ti-Nb-O film composition was linearly dependent on the pulsing ratio of the metal precursors. Obtained composition at the very low Nb:Ti pulsing ratios (<1:10) seems to produce niobium deficient films as compared to the values what linear dependency suggests (Fig. 5). According to TOF-ERDA measurements, hydrogen, carbon, and chlorine were observed as main impurities. Especially, hydrogen content was dependent on the pulsing ratio of the precursors, and increased hydrogen content was observed on the Nd rich films most probably originating from niobium ethoxide precursor (Fig. 6). The refractive index of the deposited films was almost linearly dependent on the pulsing ratio of the precursors. However, it was seen that there was some variation in the refractive index of deposited films along the precursor flow direction. Compositional difference is most likely due to the difference in the $TiCl_4/H_2O$ process deposition rate between trailing and leading edge. This is most likely due to the released HCl reacting again with the surface and thus blocking subsequent $TiCl_4$ adsorption and leading to decreased deposition rate at the downstream.[33]

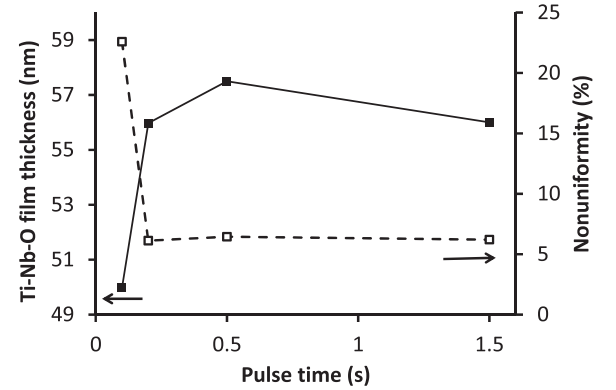

FIG. 3. Ti-Nb-O film thickness and uniformity as a function of $TiCl_4$ pulse time. Ti:Nb pulse ratio was 2:1 with 800 deposition cycles.

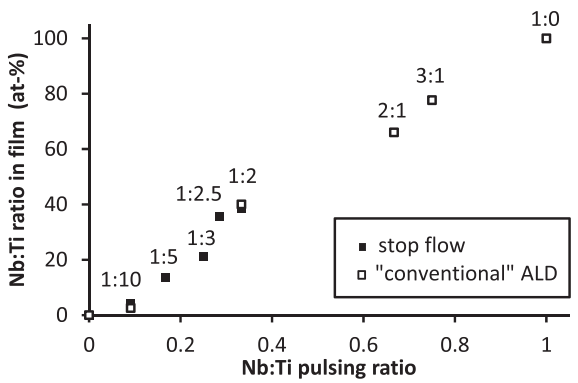

FIG. 5. Ti-Nb-O film composition as a function of precursor pulsing ratio at 175 °C.

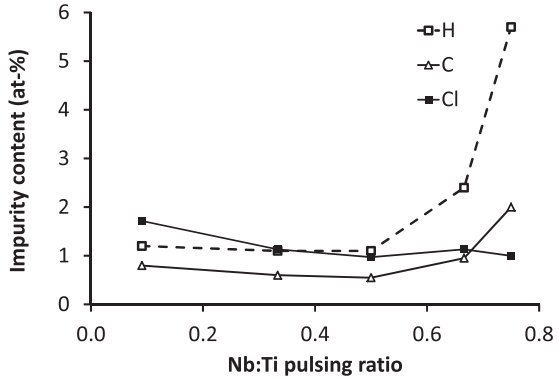

FIG. 6. Impurity levels in Ti-Nb-O thin films measured by TOF-ERDA.

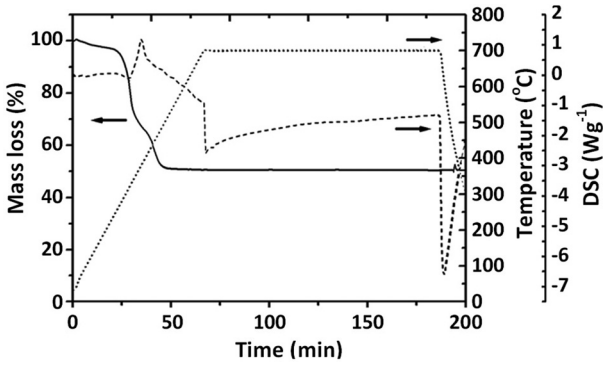

FIG. 7. TG analysis of PVA coated with Ti-Nb-O. The heating rate was 10 °C/min, and isotherms for air and 4%H_2+Ar were 10 min at 1000 °C and 2 h at 700 °C, respectively.

Ti-Nb-oxide layers were deposited onto carbon and PVA fibers with optimized pulsing and stop-flow parameters. Since the surface area of the electrospun fibers is significantly higher than the flat Si wafers used in the preliminary process evaluation, an additional stop-flow sequence was added to the deposition sequence in order to increase the precursor residence time and diffusion between the fibers. Stop-flow times between 2 and 10 s and purge times between 10 and 20 s were evaluated. It seems that the difference in the refractive index between the different sample locations decreased when at least 4.5 s stop flow time was used. A further increase in the dwell time was not improving the uniformity, and so further process evaluation was carried out by moderate length of stop-flow times between 4.5 and 6 s. It was noticed that electrospun PVA fiber mats shrank during ALD treatment leading to broken/cracked samples. Depending on the PVA composition even at 10% shrinkage was observed. Further studies indicated that thermal treatment at 60 °C or above at ambient atmosphere resulted in an increase in fiber thickness to roughly 5%–10% leading to the whole mat dimension changes.

The thermal treatment for the removal of polymer and annealing of Ti-Nb-O coating as in one process step was first carried out using thermogravimetric analysis and Ti-Nb-ratio 10:1, thickness around 50 nm, on PVA $\varnothing = 360 \pm 70$ nm). TG analyses were carried out in two atmosphere: air was used for checking the complete removal of PVA by oxidation and 4%H_2+Ar was used for removing PVA by thermal decomposition together with crystallization of Ti-Nb-O. The residual weight of the Ti-Nb-O was around 50–60 wt. % regardless of the annealing gas atmosphere (Fig. 7). The material broke down into small flakes, and thus proving that large-area tubular webs cannot be obtained. However, tubular structures with grain boundaries of crystalline Ti-Nb-O can be obtained, as shown in Fig. 8. According to XRD, a wide variety of crystal phases was found from these samples. Instead of TiO_2, the composition of Ti_3O_5 was identified, in

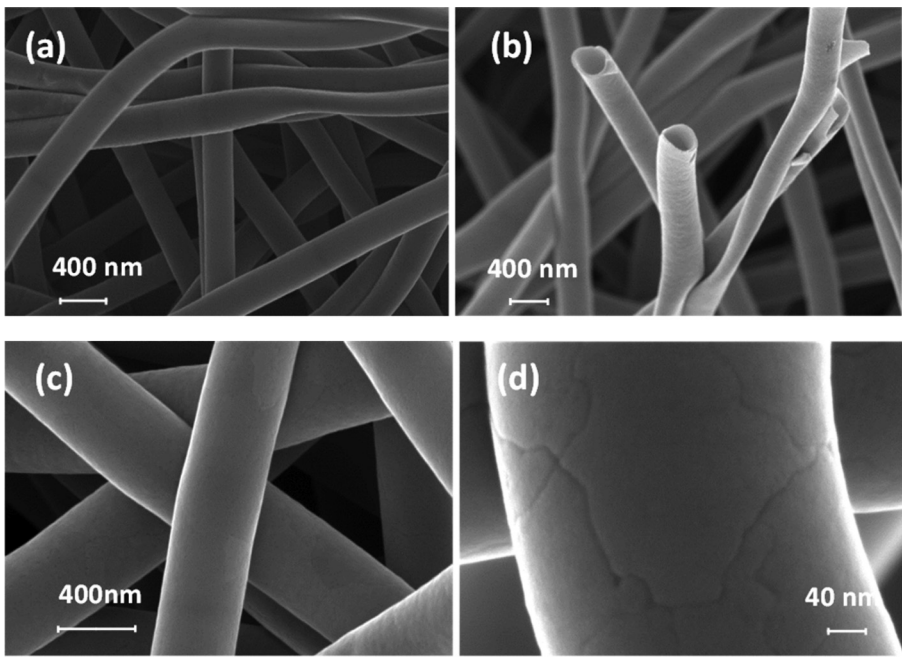

FIG. 8. Tubular support produced by thermal treatment of Ti-Nb-oxide coated PVA fibers after PVA removal (a)–(d).

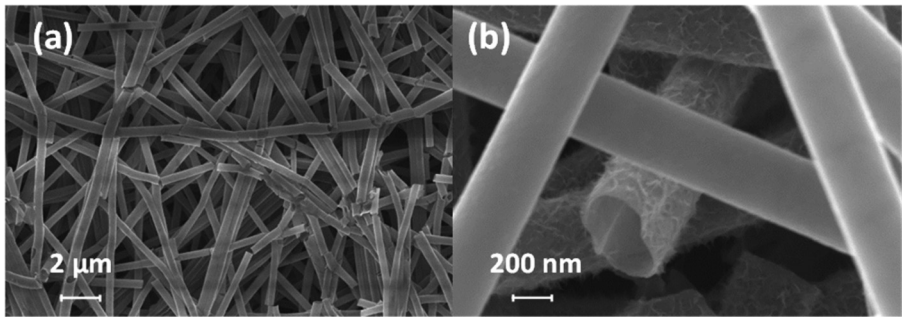

FIG. 9. SEM figures of electrospun PVA_{High}:PVA_{Low} 1:1 (14.4% solids) (a) and PVA_{High}:PVA_{Low} 2:1 (11.9% solids) (b) after Ti-Nb-O ALD and dilution in 80 °C for 30 min.

addition to niobium oxide, $Nb_{8.2}O_{21}$, and titanium niobium oxide, $Ti_{0.5}Nb_{0.5}O_2$.

In addition to thermal removal, several different dissolving conditions were evaluated for different PVA ratios to tubular Ti-Nb-O structures. Different PVA thicknesses were electrospun, followed by ALD of Ti-Nb-O. Dissolving of PVA from the ALD treated samples was tested with different temperatures between 60 and 100 °C for 30 min. Sheets of PVA fibers with Ti-Nb-oxide was broken into flakes during PVA removal, regardless of the temperature or ramping time used. Dissolution of Ti-Nb-oxide coated PVA fibers had slight surface patterning on the tube walls (Fig. 9). In our earlier work, we have obtained coral-like complex tube walls using PVA template fibers with Al_2O_3 coatings and dissolution for template removing,[34] but this type of behavior was not observed.

Further studies were concentrated on the ALD onto carbon fibers since the tubular Ti-Nb-O structures were too fragile to produce conductive sheets of support materials. Therefore, ALD studies were concentrated onto depositions to carbonized sheets with thicknesses ranging from 10 to 30 μm. Although the core–shell carbon oxide fiber sheets were more fragile than the uncoated carbon sheets, they fractured easily and, e.g., tensile test of the sheets was not possible, they still remained in the sheet form, thus enabling further treatments, e.g., thermal treatments and ALD of Pt. The appearance of uncoated and coated fibers is shown in Fig. 10. The as-deposited films had smooth texture whereas the crystal grains and larger structures were visible in the annealed fibers. Once Nb:Ti ratio was changed from 0:1 to 1:1, the increased Nb-content shifted the d-value of (101) peak from 3.50 to 3.55. The evolution of the crystalline structure can be seen in the SEM images in Fig. 10. Two dimensional, flat crystalline grains are visible when the thickness of the film is around 30 nm, while in other images [Figs. 10(c) and 10(d)], grainy structure is clearly visible from samples with a film thickness around 70 nm. The increase in the grain growth during annealing might be linked to previously reported rapidly proceeding crystallization of Ti-Nb-O films.[19]

XRD measurements were performed for as-deposited and annealed Ti-Nb-O films on fibrous samples. The

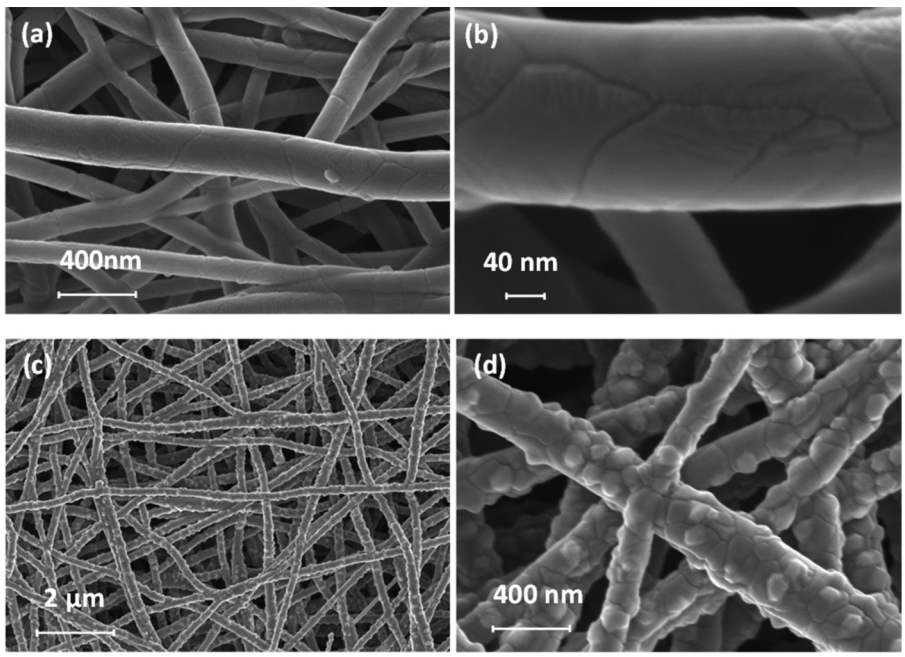

FIG. 10. Annealed carbon-ceramic core shell fiber with a 30 nm Ti-Nb-O [(a), (b)] and 70 nm [(c), (d)] thick coating.

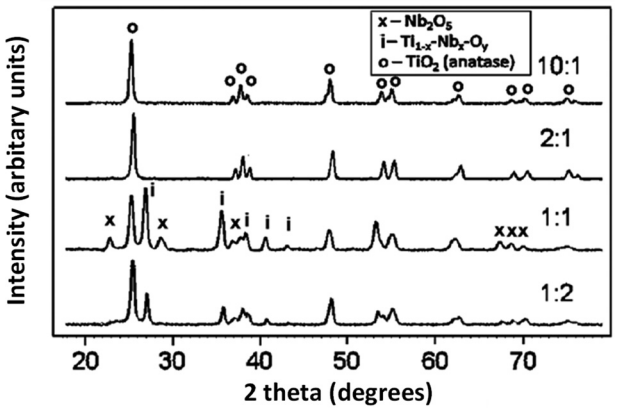

FIG. 11. X-ray diffraction patterns of annealed Ti-Nb-O films as a function of Ti:Nb precursor pulsing ratio.

as-deposited films were already slightly crystalline (Fig. 11). It can be seen that the small intensity (101) anatase type TiO_2 was observed as a preferred orientation for samples with low niobium content. On Nb-rich samples, $Ti_{0.5}Nb_{0.5}O_2$ and Nb_2O_5 can also be identified when the Nb:Ti pulsing ratio is 1:1 or 2:1. Annealing under forming gas at 700 °C increased the film crystallinity. After annealing, however, crystalline Nb_2O_5 was not found even from Nb rich sample deposited with 1:1 Ti:Nb ratio. TiO_2 anatase (101) peak was the most intense whereas peaks originating from $Ti_{0.5}Nb_{0.5}O_2$ and Nb_2O_5 almost disappears, indicating solid state reaction with TiO_2. Crystallization of ALD films as function of annealing temperature was studied by *in situ* high temperature XRD. In these measurements, the films were annealed and XRD measurements were repeatedly carried out up to 900 °C. It was found that precursor pulsing ratios affects the obtained crystal structures and the temperature where crystallization increased (Figs. 12 and 13). An increase in crystallization onset of samples with low niobium content is observed at around 375 °C whereas samples with 1:1 Ti:Nb pulsing ratio required 650 °C for crystallinity to increase.

Conductivities of core–shell fiber sheets play a critical role when these types of structures are being considered as electrocatalyst support materials. Carbon itself has a relatively good conductivity of around 5–20 S cm^{-1},[35] but the

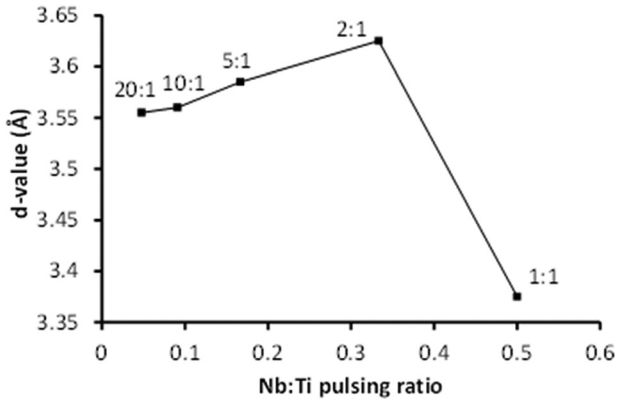

FIG. 12. d-value of anatase (101) reflection as a function of precursor pulsing ratio.

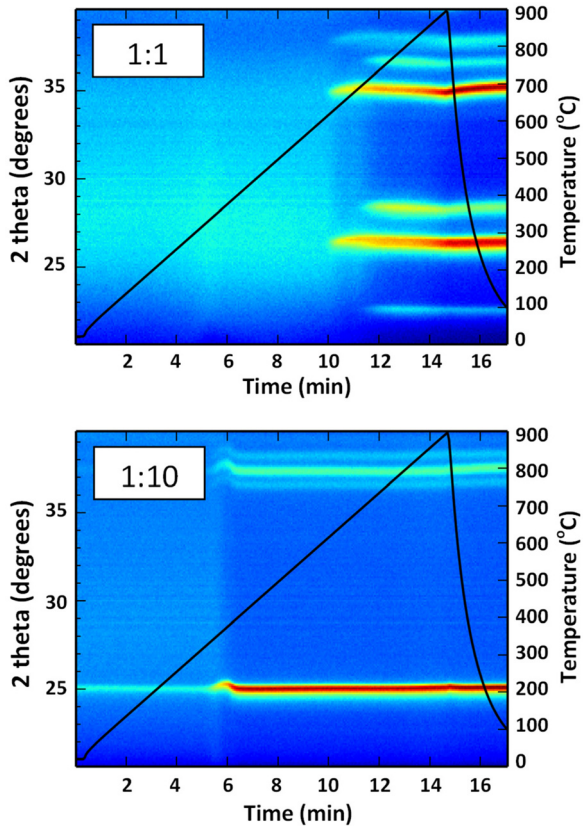

FIG. 13. (Color online) *In situ* XRD on Ti-Nb-O film from room temperature up to 900 °C.

protective oxide layer must be conductive as well to meet the PEM fuel cell requirements of 10^{-2} S/cm.[36] In-plane conductivities of the ALD Ti-Nb-O on reference borosilicate glass as well as on carbon fiber sheets were measured by a four-point probe with barrel-type probes having a relatively large curvature of contact point with 5 mm distance between the probes.[20] The determination of conductivity of Ti-Nb-oxide coating with this set-up was proven challenging, as can be seen from large variation between measurements. However, as expected, as deposited Ti-Nb-O was insulating but annealing at 700 °C in forming gas turned oxide materials conducting. According to the four-point probe measurements conductivities were at the same level that of the uncoated carbon fiber sheets (Table II). The highest conductivities on insulating borosilicate glass seems to be obtained from samples having Ti:Nb pulsing ratios of 5:1 or greater.

TABLE II. Conductivities of annealed ALD layer on carbon fiber sheets and reference borosilicate.

Ti-Nb pulsing ratio	Thickness (nm)	Conductivity on carbon (S/cm)	Conductivity on borosilicate (S/cm)
10:1	77	4.6–5	3.7–52
5:1	61	—	1–2.3
3:1	47	—	0.6–1
2:1	45	14–18	0.5–0.9
1:1	54	17–20	0.2–0.4
1:2	67	11–14	0.2

IV. CONCLUSIONS

Ti-Nb oxide layers have been successfully deposited onto carbonized and polymeric electrospun fibers for the preparation of core–shell fibrous and tubular structures. Annealed carbon core, oxide shell fiber mats remained in their sheet form and had similar conductivity as the support carbon without the oxide layer. The tubular structure obtained from annealing of polymer core, oxide shell materials produced flakes composing of tubular materials since PVA polymer was pyrolyzed during the annealing process. The demonstrated preparation routes for the core–shell carbon fiber mats and tubular Ti-Nb-O flakes provide interesting route for subsequent platinum deposition and possible applications as support structures for catalyst applications in fuel cells.

ACKNOWLEDGMENTS

This paper is based on results from the CATAPULT project. CATAPULT (2013–2016) was funded by the European Commission and Fuel Cell and Hydrogen Joint Undertaking (Grant Agreement No. 325268), and by the Finnish Funding Agency for Technology and Innovation TEKES. Funding from the Academy of Finland (Project ID 263 577) is also gratefully acknowledged.

[1]S. Zhang, Y. Shao, G. Yin, and Y. Lin, J. Mater. Chem. A **1**, 4631 (2013).
[2]Y. Y. Shao, G. P. Yin, Y. Z. Gao, and P. F. Shi, J. Electrochem. Soc. **153**, A1093 (2006).
[3]H. Chhina, S. Campbell, and O. Kesler, J. Power Sources **161**, 893 (2006).
[4]Y. Zhong, X. Xia, F. Shi, J. Zhan, J. Tu, and H. J. Fa, Adv. Sci. **3**, 1500286 (2016).
[5]M. S. Saha, R. Y. Li, and X. L. Sun, Electrochem. Commun. **9**, 2229 (2007).
[6]M. N. Saha, R. Y. Li, M. Cai, and X. L. Sun, Electrochem. Solid State. Lett. **10**, B130 (2007).
[7]Y. Suzuki, A. Ishihara, S. Mitsushima, N. Kamiya, and K. I. Ota, ECS Solid State Lett. **10**, B105 (2007).
[8]M. C. Orilall, F. Matsumoto, Q. Zhou, H. Sai, H. D. Abruna, F. J. DiSalvo, and U. Wiesner, J. Am. Chem. Soc. **131**, 9389 (2009).
[9]L. Zhang, L. Y. Wang, C. M. B. Holt, T. Navessin, K. Malek, M. H. Eikerling, and D. Mitlin, J. Phys. Chem. C **114**, 16463 (2010).
[10]S. Y. Huang, P. Ganesan, and B. N. Popov, Appl. Catal. B **102**, 71 (2011).
[11]S. L. Gojković, B. M. Babić, V. R. Radmilović, and N. V. Krstajić, J. Electrochem. Soc. **639**, 161 (2010).
[12]S. Sun, G. Zhang, X. Sun, M. Cai, and M. Ruthkosky, J. Nanotechnol. **2012**, 389505 (2012).
[13]Y. Shao, J. Sui, G. Yin, and Y. Gao, Appl. Catal. B **79**, 89 (2008).
[14]H. Meng and P. K. Shen, J. Phys. Chem. B **109**, 22705 (2005).
[15]Z. D. Wei, M. B. Ji, Y. Hong, C. X. Sun, S. H. Chan, and P. K. Shen, J. Power Sources **160**, 246 (2006).
[16]L. Zhang, L. Wang, C. M. B. Holt, B. Zahiri, Z. Li, K. Malek, T. Navessin, M. H. Eikerling, and D. Mitlin, Energy Environ. Sci. **5**, 6156 (2012).
[17]R. S. Hsu, D. Higgins, and Z. Chen, Nanotechnology **21**, 165705 (2010).
[18]C. Marichy and N. Pinna, Coord. Chem. Rev. **257**, 3232 (2013).
[19]V. Pore, M. Ritala, M. Leskelä, T. Saukkonen, and M. Järn, Cryst. Growth Des. **9**, 2974 (2009).
[20]P. Heikkilä *et al.*, "Core-shell Carbon-Ti-Nb-O fibres with Pt thin films as catalysts for PEM fuel cell MEAs" (unpublished).
[21]M. Putkonen, T. Sajavaara, L. Niinistö, and J. Keinonen, Anal. Bioanal. Chem. **382**, 1791 (2005).
[22]H. J. Whitlow, G. Possnert, and C. S. Petersson, Nucl. Instrum. Methods B **27**, 448 (1987).
[23]J. F. Ziegler, "SRIM," http://www.SRIM.org, 2006.
[24]"SIMNRA simulation program," www.rzg.mpg.de/~mam.
[25]M. Bognitzki, H. Hou, M. Ishaque, T. Frese, M. Hellwig, C. Schwarte, A. Schaper, J. H. Wendorff, and A. Greiner, Adv. Mater. **12**, 637 (2000).
[26]"IMAGEJ," http://imagej.nih.gov/ij/.
[27]K.-E. Elers, M. Ritala, M. Leskelä, and E. Rauhala, Appl. Surf. Sci. **82/83**, 468 (1994).
[28]K. Knapas, A. Rahtu, and M. Ritala, Chem. Vap. Deposition **15**, 269 (2009).
[29]K. Kukli, M. Ritala, M. Leskelä, and R. Lappalainen, Chem. Vap. Deposition **4**, 29 (1998).
[30]M. Putkonen, ECS Trans. **25**, 143 (2009).
[31]J. W. Elam and S. M. George, Chem. Mater. **15**, 1020 (2003).
[32]A. Kosola, M. Putkonen, L.-S. Johansson, and L. Niinistö, Appl. Surf. Sci. **211**, 102 (2003).
[33]M. Ritala, M. Leskelä, E. Nykänen, P. Soininen, and L. Niinistö, Thin Solid Films **225**, 288 (1993).
[34]P. Heikkilä, T. Hirvikorpi, H. Hilden, J. Sievänen, L. Hyvärinen, A. Harlin, and M. Vähä-Nissi, J. Mater. Sci. **47**, 3607 (2012).
[35]P. Heikkilä, A. Pasanen, S. Virtanen, K. Polak-Krasna, and M. Vähä-Nissi, "Electrospinnability and properties of electrospun fibres and sheet from CA, PLLA, PES, and PAN" (unpublished).
[36]B. C. H. Steele and A. Heinzel, Nature **414**, 345 (2001).